Protein–protein interaction as a powering source of oxidoreductive reactivity†

Tiao-Yin Lin*

Received 5th January 2010, Accepted 24th March 2010
First published as an Advance Article on the web 17th May 2010
DOI: 10.1039/b927132e

Thiol-disulfide exchange reactions between thiol-disulfide oxidoreductases (*e.g.* thioredoxin or Trx) and client proteins can obtain a rate several orders faster than those between chemical reagents (*e.g.* dithiothreitol) and client proteins. The active sites of these oxidoreductases are characterized by a CXXC motif. The XX dipeptide of Trx is GP. By altering the C-terminal X to A, K and D, it is shown that the P → K mutation confers the largest effect on the redox potential, which it elevated by 28 mV, while the P → D mutation displays the smallest variation. The change in pK_a of the nucleophilic thiol also follows this trend. However, GK and GA react faster with thioredoxin reductase, exhibiting a rate rank of GK > GA > GP > GD, while the rates toward insulin and PDI follow the order GP > GA > GK > GD. The rate change spans two to three orders of magnitude. This work demonstrates that redox reactivity does not correlate simply with pK_a and redox potential, but instead supports the important role of interaction between proteins in determining the fast reactivity and rate order of Trx. A reaction mechanism involving the transient formation of a Trx–protein binding complex is proposed for the oxidoreduction of protein thiols-disulfides. Furthermore, studies on insulin reduction show that Trx acts as an enzyme rather than a redox couple. These results provide explanations for the observed variations of the CXXC motif in PDI-like proteins as well as the conservation of the CXXC motif in Trx.

Introduction

Thiol-disulfide oxidoreductases of the thioredoxin (Trx) superfamily play a pivotal role in numerous biological and disease processes.[1,2] Oxidoreduction of protein thiol/disulfide performed by these enzymes can achieve a rate several orders of magnitude faster than that by chemical reagents, such as dithiothreitol (DTT) and glutathione.[3,4] The fast rate is crucial for biological redox processes in organisms, but the reason for the high reactivity has not been fully determined.

The structures of these thiol-disulfide oxidoreductases are highly homologous and are characterized by a CXXC motif in the redox active site of the Trx fold.[5] The XX dipeptide is a crucial determinant of redox potential ($E^{o\prime}$).[6,7] $E^{o\prime}$ varies from −270 mV for *E. coli* Trx, near −175 mV for protein disulfide isomerase (PDI), to −120 mV for *E. coli* DsbA.[8–11] Variations of enzyme activities were commonly attributed to the changes of $E^{o\prime}$, which is influenced by the XX dipeptides. But the CXXC motif is more than a determinant of $E^{o\prime}$.[12] It was also reported that the XX dipeptide affects the pK_a of the nucleophilic Cys of the CXXC motif, and the N-terminal X position of the dipeptide in *E. coli* Trx affects interactions between proteins.[13,14] As the dipeptide is altered, all these factors vary simultaneously, and identifying a specific cause for the observed enzyme activities remains a challenge.

The CXXC motif is conserved in thiol-disulfide oxidoreductases. The canonical CXXC motif is CGPC in Trx, and CGHC in PDI. Nevertheless, drastic changes were observed in a transmembrane member of yeast PDI-like protein Eps1, which mediates substrate recognition in ER-associated degradation (ERAD).[15] Eps1 contains two Trx-like domains with active site sequences CPHC and CDKC. Charged residues in the C-terminal X are also found in two PDI-like proteins devoid of the nucleophilic Cys in the CXXC motif: in a human transmembrane PDI, TMX2, and a human testis specific PDI, PDILT,[16,17] which exhibit SNDC and SKKC sequences, respectively. The significance of the replacements is unclear.

In this study, the C-terminal X of the $CX_{33}X_{34}C$ motif in *E. coli* Trx was mutated to generate a neutral P34A, a negatively-charged P34D, or a positively-charged P34K mutant. The effects of the variations on pK_a of the nucleophilic Cys, $E^{o\prime}$, and reactions with various target proteins were investigated.

Trx participates in the preservation of the reduced states of cytoplasmic proteins and cellular redox homeostasis. In cells, NADPH reduces Trx using Trx reductase (TrxR) as a catalyst. Reducing equivalents are transferred from NADPH, *via* FAD, to redox active cysteines of TrxR, and then to Trx.[18] Mutation of Pro_{34} of *E. coli* Trx to His to mimic the active site of PDI resulted in a higher $E^{o\prime}$ and an increase of activity with TrxR.[8] How other mutations at the Trx C-terminal X position will affect $E^{o\prime}$ and activity with TrxR is an interesting question.

Trx reduces insulin with a rate four orders of magnitude higher than that of DTT.[3] The origin of the exceptional reactivity is not clear. Insulin has been used as a model substrate for an oxidoreductase, and differences in activities among variants of the oxidoreductase are often attributed to $E^{o\prime}$.[19–21]

Department of Biological Science and Technology, National Chiao Tung University, 75 Poai St., Hsinchu, Taiwan, Republic of China. E-mail: tylin@cc.nctu.edu.tw

† Electronic supplementary information (ESI) available: Fig. S1 and S2. See DOI: 10.1039/b927132e

However, reducing activity does not always agree with $E^{o\prime}$,[21,22] and what controls the activities in the reduction of insulin is still elusive.

PDI is a multidomain redox protein catalyzing protein folding by the formation and isomerization of disulfides.[2] PDI has four Trx-like domains, *a*, *b*, *b*′ and *a*′.[23] The protein carries out oxidoreduction through its redox active CGHC motif in *a*- and *a*′-domains.[23] PDI increases the rate of the oxidation of β-lactamase by 500-fold, and the rate of the oxidative folding of bovine pancreatic trypsin inhibitor (BPTI) folding intermediates by 3000–6000-fold.[4,24] Humans have 19 PDI-like proteins, with different CXXC motifs and domain composition.[2] Further investigations are required to understand the necessity of the diversity.

The wild-type and mutants investigated here provide insights into the relation between C-terminal X and $E^{o\prime}$, pK_a, substrate specificity, as well as the redox reaction rate. It shows that redox activity does not correlate simply with $E^{o\prime}$ or pK_a, and supports a crucial role of interaction between a redox protein and its target protein. This latter effect can potentially dominate those of $E^{o\prime}$ or the nucleophilic pK_a, and explains several hitherto puzzling phenomena that can not be understood in terms of $E^{o\prime}$. The interaction between proteins not only provides the target recognition but also powerfully accelerates the reaction. The acceleration underlies the origin of the exceptional reactivity of Trx in reducing insulin, and the efficiency of PDI in thiol-disulfide exchange. Analysis of insulin reduction in the Trx system reveals that Trx behaves as an enzyme rather than a redox couple. A revised reaction mechanism for oxidoreduction of protein thiols-disulfides by Trx is proposed.

Results

Construction of Trx variants and physical characterizations

The role of the C-terminal X of CXXC motif in $E^{o\prime}$, pK_a, and redox kinetics was investigated using the archetype thiol-disulfide oxidoreductase, *E. coli* Trx. Mutations of Pro34 in the $C_{32}GPC_{35}$ active site of Trx to Asp, Ala and Lys yielded P34D, P34A and P34K mutants. The expression level of the mutant proteins was not significantly affected. They migrated to the same position on SDS-PAGE as the wild-type (Fig. 1A). However, on the native non-reducing PAGE, P34D migrated faster, while P34K slower, relative to the wild-type (Fig. 1B). Fluorescence spectra of the oxidized mutants are identical to that of the wild-type (Fig. 1C). Upon reduction, the intensity of mutant proteins increases; the magnitude is close to the change of the wild-type, suggesting that the mutant proteins are structurally similar to the wild-type.

Redox potential

$E^{o\prime}$ of the wild-type, P34D, P34A, and P34K mutants were determined by redox equilibration with glutathione.[9] The measured redox equilibrium constant (*K*) for the wild-type was 10 ± 1 M, equivalent to $E^{o\prime}$ of -270 ± 1 mV (Table 1). *K* for P34D, P34A and P34K mutants decreased 3.4-fold, 4.5-fold, and 8.3-fold, respectively. $E^{o\prime}$ of P34D and P34A increased 16 mV and 20 mV, respectively. The P34K mutant had the most oxidative power, 28 mV more than the wild-type. These results show that all mutations significantly affect $E^{o\prime}$. The effect of Lys is the largest, and that of Asp is smaller than that of Ala.

Table 1 Redox equilibrium constant (*K*), $E^{o\prime}$, and pK_a of Trx. *K* was measured using glutathione as a reference. pK_a was obtained from titration of the nucleophilic Cys.

	K M	$E^{o\prime}$ mV	pK_a
WT	10 ± 1	-270 ± 1	7.6 ± 0.1
P34D	2.9 ± 0.3	-254 ± 1	6.7 ± 0.1
P34K	1.2 ± 0.1	-242 ± 1	5.5 ± 0.1
P34A	2.2 ± 0.2	-250 ± 1	6.6 ± 0.1

pK_a of the nucleophilic cys

The extinction coefficient of absorbance at 240 nm (ε_{240}) increases when a thiol deprotonates. Therefore, pK_a of the nucleophilic Cys of Trx was investigated by monitoring the pH-dependent change of ε_{240}. Plotting ε_{240} against pH yielded a pK_a of 6.7, 6.6, and 5.5 for P34D, P34A, and P34K Trx, respectively, whereas the wild-type exhibited a titration pattern that was consistent with a pK_a of 7.6 (Fig. 2, Table 1). The large decrease of pK_a in P34K suggests a stabilization effect of the positively charged Lys at the C-terminal X on the nucleophilic thiolate. P34D, on the contrary, has only slightly increased pK_a of Cys compared to P34A.

Rate of reduction of Trx variants catalyzed by TrxR

The effects of the C-terminal X on the redox reactivity were investigated by reactions between Trx and several proteins. Trx is catalytically reduced by TrxR using NADPH as a reducing equivalent.[18] The measurements show that the wild-type Trx was reduced with a high catalytic efficiency (k_{cat}/K_m) of 878 μM^{-1} min^{-1} (Fig. 3, Table 2). P34K and P34A mutations increased the catalytic efficiency by 2.3-fold and 1.4-fold, respectively. The alteration is mostly due to the reduction of K_m. In contrast, TrxR displayed a catalytic efficiency on P34D only 4.5% of the wild-type. Similarly, the k_{cat} was not decreased; instead, the effect was totally attributed to K_m, which increased by 24-fold. The order of redox activity matches K_m but not $E^{o\prime}$ or pK_a when comparing the wild-type and the three mutants, indicating that the interaction between proteins predominates over the effects of $E^{o\prime}$.

In computer simulations of TrxR catalyzed reduction of Trx, Glu38 of TrxR is 6.47 Å away from Pro34 of the wild-type Trx (Fig. 4A). Lys34 of the P34K mutant can interact favorably with the Glu38 (Fig. 4B). The decrease of K_m for the P34A suggests the mutant also interacts better with TrxR (Fig. 4D). In contrast, repulsion between Asp34, in the P34D mutant, and the Glu38 (Fig. 4C) results in a high K_m.

Reduction of insulin by Trx

The activity of Trx in insulin reduction was investigated by stoichiometric oxidoreductive reactions. Reduction of insulin by wild-type Trx was much faster than by P34D and P34K mutants (Fig. 5). Within one minute of the reaction, approximately 89.4%, 59%, 17.4%, and 1.4% of the wild-type, P34A,

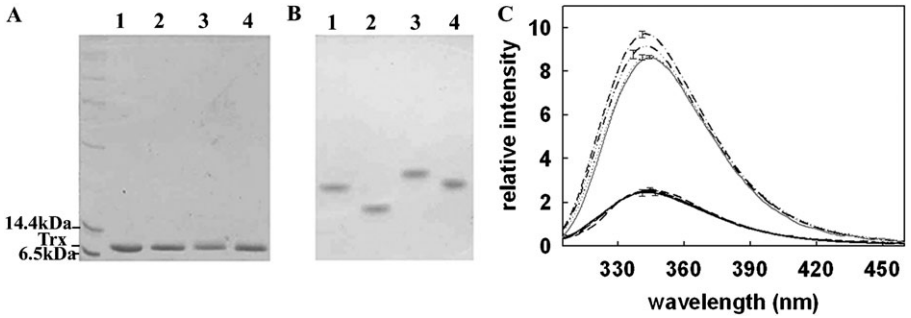

Fig. 1 Physical properties of P34D, P34A and P34K mutants. (A) SDS-PAGE of the purified P34K (lane 1), P34D (lane 2), wild-type Trx (lane 3), P34A (lane 4). (B) Native PAGE of the purified wild-type (lane 1), P34D (lane 2), P34K (lane 3), and P34A (lane 4). (C) Fluorescence spectra of the wild-type and mutant Trx. The spectra of 7 μM Trx, 0.05 M sodium phosphate, pH 7.5, were taken at 25 °C. The spectra are the averages of three independent experiments, and the ranges of variations are indicated by bars. Reduced wild-type (·····), reduced P34K (–·–·–), reduced P34D (–··–··–), oxidized wild-type (—), oxidized P34K (— —), oxidized P34D (- - - -), oxidized P34A (– – –), reduced P34A (——). The four oxidized spectra are mostly overlapping.

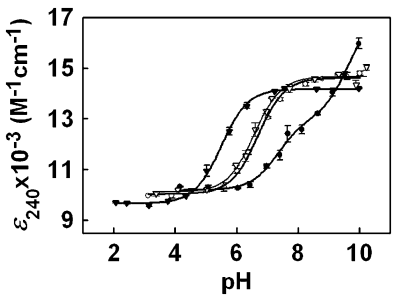

Fig. 2 Ionization of the nucleophilic thiols of Trx. ε_{240} of the wild-type (●), P34D (○), P34K (▼), P34A (▽) mutant Trx are plotted as a function of pH. The data of P34D, P34K, and P34A Trx were fitted with a single group titration curve. The complex wild-type titration behavior was fitted to the curve for two interacting monoprotic species, Cys32 and Asp26 of Trx.[38]

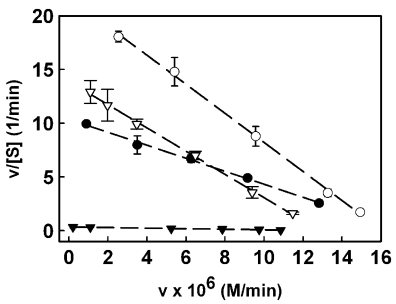

Fig. 3 TrxR catalyzed reduction of Trx. The kinetics of TrxR catalyzed reduction of Trx graphed in an Eadie–Hofstee plot. Linear regressions are shown by dashed lines. The reaction contains 5.4 nM of TrxR, and Trx concentration was varied. (●), wild-type Trx, (○), P34K, (▼), P34D, (▽), P34A.

P34K, and P34D Trx were oxidized, respectively. The second order rate constant, k_{app}, was 1.4×10^5 M^{-1} s^{-1} for the wild-type, and decreases 5.8-fold, 40-fold and 583-fold for the P34A, P34K and P34D mutants, respectively (Table 3). The results demonstrate that a single charged residue in the active site of Trx can drastically decrease its activity toward insulin. Such change is not dictated by $E^{o\prime}$ or pK_a, since their

Table 2 Kinetic parameters of TrxR catalyzed reduction of Trx. Reduction of Trx by 0.24 mM NADPH was catalyzed by 5.41 nM TrxR at pH 7.

	K_m μM	k_{cat} min^{-1}	k_{cat}/K_m μM^{-1} min^{-1}
WT	1.62 ± 0.03	1422 ± 115	878 ± 72
P34D	38.0 ± 1.6	1535 ± 184	40.4 ± 5.1
P34K	0.73 ± 0.02	1499 ± 68	2041 ± 113
P34A	1.06 ± 0.1	1266 ± 75	1194 ± 133

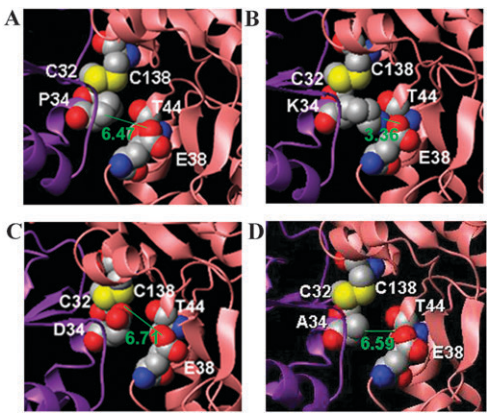

Fig. 4 Interaction of TrxR with Trx near position 34 of Trx. Ribbon diagram showing locations of C32 and position 34 in the wild-type Trx (purple) (A), P34K mutant (B), P34D mutant (C), and P34A mutant (D) relative to C138, E38, and T44 of TrxR (coral) in the complex structure.[18] Residues are displayed by the CPK model. C, O, N, and S atoms are colored grey, red, blue, and yellow, respectively. Distances between indicated atoms are shown in green.

alterations are largest for the P34K mutant, while the greatest change in activity arises from P34D mutation.

Insulin reduction using the Trx system

To further investigate the factor that influences reduction rate, insulin was reduced by the Trx system, which is composed of NADPH, TrxR and Trx. The wild-type Trx reduced insulin with an apparent K_m of 10.3 μM and k_{cat} of 57 min^{-1}

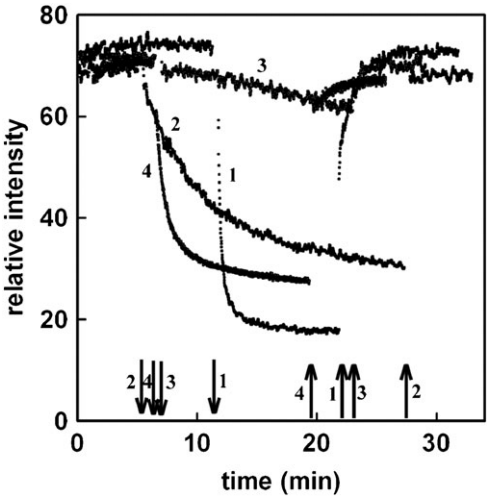

Fig. 5 Reduction of insulin by Trx. Reduction of insulin by Trx was monitored by fluorescence. The reaction mix contained 1 μM reduced Trx, and insulin was added to the same concentration (indicated by a down arrow). Finally, DTT was added to 1 mM (up arrow). The numbers 1, 2, 3, and 4 indicate the wild-type, P34K, P34D, and P34A.

Table 3 Rate constants of stoichiometric redox reactions. Rate constants were obtained from stoichiometric reactions at pH 7 for the reduction of insulin by Trx (left column) and oxidation of Trx by PDI (right column).

	Reduction of insulin k_{app} M^{-1} s^{-1}	Oxidation of Trx k_{app} M^{-1} s^{-1}
WT	$(1.4 \pm 0.3) \times 10^5$	$(6.3 \pm 0.6) \times 10^3$
P34D	$(2.4 \pm 0.1) \times 10^2$	$(4.2 \pm 0.3) \times 10^2$
P34K	$(3.5 \pm 0.3) \times 10^3$	$(1.5 \pm 0.2) \times 10^3$
P34A	$(2.4 \pm 0.2) \times 10^4$	$(4.7 \pm 0.2) \times 10^3$

(Fig. 6, Table 4). In comparison, P34A′s K_m was 17.1 μM and k_{cat} was 41 min^{-1}, while P34K′s K_m was approximately 57.5 μM and k_{cat} was 15 min^{-1}. The efficiency of reduction catalyzed by the wild-type was 2.3-fold and 21-fold higher than those by P34A and P34K Trx, respectively, consistent with the effect observed in the stoichiometric reaction. The amount of insulin reduced by P34D was too low to be detected, which was consistent with the huge (583-fold) effect seen in the stoichiometric reaction. Nevertheless, the difference in K_m between the wild-type and P34A and P34K reveals that the interaction of Trx with insulin is a crucial factor for the rapid redox reactivity, and these mutations hamper the interaction.

Insulin has three disulfides (Fig. 7B).[25] The first A_C7–B_C7 disulfide (between A chain C7 and B chain C7) is hydrophobic (Fig. 7A and C), the nearest charge at A_E4 carboxylate being 8.67 Å away. The surface accessibility measured with a sphere of 1.4 Å indicates that A_C7–B_C7 is the most accessible (52% for the sulfur of A_C7, and 18% for that of B_C7). Therefore, this hydrophobic disulfide is accessible and is reduced rapidly by the wild-type and P34A Trx; however, it reacts poorly with the other two mutants. The surroundings of the second A_C6-A_C11 disulfide are enriched with nonpolar residues (Fig. S1A†), while the third A_C20-B_C19 disulfide contacts with two charged residues

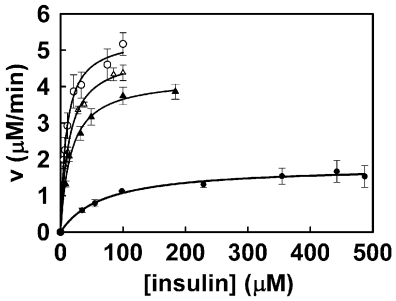

Fig. 6 Insulin reduction using the Trx system. The system consisted of 0.1 μM of wild-type Trx (○), P34K (●) or P34A (▲), 0.11 μM TrxR, and 0.4 mM NADPH. An experiment performed under the same condition but with 0.2 mM NADPH for the wild-type Trx is also shown (△). Michaelis–Menten fits are shown by solid curves.

Table 4 Kinetic constants for the reduction of insulin catalyzed by the Trx system Experiments were performed in 0.4 mM NADPH, 0.11 μM TrxR, and 0.1 μM Trx as described in the Experimental.

	K_m μM	V_m μM min^{-1}	k_{cat} min^{-1}	k_{cat}/K_m μM^{-1} min^{-1}
WT	10.3 ± 2.0	5.7 ± 0.4	57 ± 4	5.53 ± 1.14
P34K	57.5 ± 8.8	1.5 ± 0.4	15 ± 4	0.26 ± 0.08
P34A	17.1 ± 0.9	4.1 ± 0.1	41 ± 1	2.40 ± 0.14

(Fig. S1B†). Although the latter disulfide might be reactive toward P34K and P34D Trxs, measurement of surface accessibility showed that both disulfides are barely accessible.

Oxidation of Trx variants by PDI

PDI was shown to react with Trx.[26] Here, the mutant and wild-type Trx were used to study the substrate preference of PDI. Oxidation of Trx by PDI was investigated by a stoichiometric redox reaction. The oxidized and the reduced PDI displayed practically identical fluorescence intensity (Fig. 8A). The oxidation of the reduced Trx by PDI was monitored by the decrease of the fluorescence intensity. The reactivity followed a rank of wild-type > P34A > P34K > P34D (Fig. 8B). The apparent rate constant was 6.3×10^3 M^{-1} s^{-1} for the wild-type, and decreased 1.3-fold, 4.2-fold and 15-fold for P34A, P34K and P34D, respectively (Table 3). The reaction was not studied using the Trx system because PDI also significantly reacts with TrxR.[26] However, the order of reactivity of Trx with PDI is not compatible with the rank of $E^{o\prime}$ or pK_a, but is identical to that of insulin reduction by Trx, suggesting that the mechanism of protein–protein interaction dominates the reactivity. This view is further supported by structural analysis as follows.

Affinity of peptides toward PDI was found to depend on the peptide length, with peptides of 30 residues being better than shorter ones.[27] Also, heptameric peptides containing a sequence of small/helix breaker-cysteine-X-hydrophobic/basic-hydrophobic had higher affinities.[28] PDI has a largely hydrophobic environment near both redox active sites (Fig. 9A and B). Here, using a protein as substrate for PDI, it was found that the wild type with a more hydrophobic residue at the C-terminal X reacts better than P34A, which in turn is better than a positively charged P34K. The negatively-charged

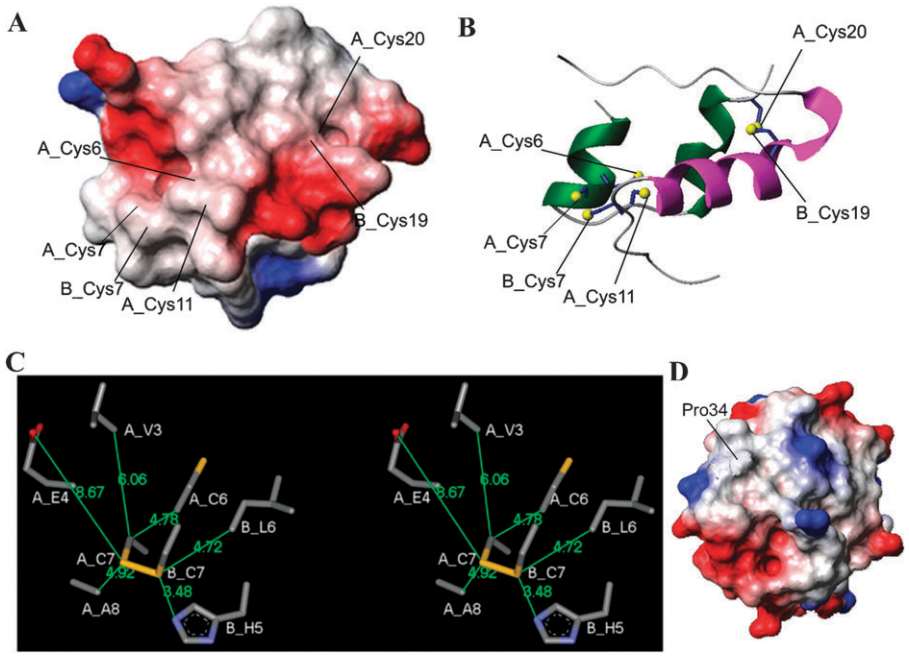

Fig. 7 Features of the surroundings of insulin disulfides. Electrostatic potential surface map (red, acidic; white, neutral; blue, basic) (A), ribbon diagram showing cysteine positions (B), and stereo view showing neighbors of A_C7–B_C7 disulfides and contact distance (C) for bovine insulin (20). In (B), helices are dark green for A chain, magenta for B chain. Only side chains of cysteines are depicted with sulfur atoms in yellow spheres. (D) Surface electrostatic potential for Trx.[5]

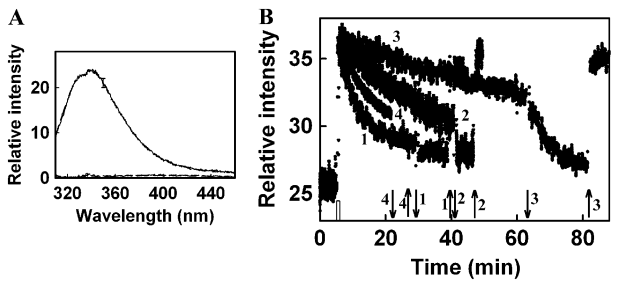

Fig. 8 Oxidation of Trx by PDI. (A) Fluorescence spectra of 0.5 μM PDI or 1 μM insulin in 0.1 M sodium phosphate, 2 mM EDTA, pH 7. The spectra of the reduced proteins were recorded in the presence of 1.5–2 mM DTT. Oxidized (——) and reduced (— —) PDI spectra are essentially overlapping. Oxidized (– – –) and reduced (- - - -) insulin spectra have very low relative intensity. (B) PDI-mediated oxidation of Trx followed by fluorescence. The reaction mix initially consisted of 0.5 μM PDI. Reduced Trx was added to 0.5 μM (vertical bar), followed by insulin to 0.33 μM to oxidize the remaining Trx (down arrow). Finally, DTT was added to 2 mM (up arrow). The numbers 1, 2, 3, and 4 indicate the curves for the wild-type, P34K, P34D, and P34A Trx, respectively.

P34D is the worst one due to the hydrophobic redox environments of PDI and also the presence of a negatively-charged Glu49 near Cys58 of the *a*-domain (5.49 Å) (Fig. 9A). These findings suggest that the diversity of PDI-like proteins is necessary for achieving efficient interaction with different substrate proteins.

Discussion

pK_a of the nucleophilic Cys

The thiolate of the nucleophilic Cys in the CXXC is stabilized by the partial positive charge of the α2 helix dipole in the wild-type Trx, resulting in a pK_a (= 7.6) lower than the normal Cys.[29] The P34A, P34K and the P34D mutations further decreased the pK_a of Cys32 of Trx by approximately one to two units. These mutations allow the formation of a hydrogen bond between the amide nitrogen of the C-terminal X and the sulfur of Cys32.[30] P34A lowers the pK_a by one unit, corresponding to a 1.4 kcal mol^{-1} stabilization energy due to the amide hydrogen bonding. The low pK_a of P34K gives the largest stabilization energy of 2.9 kcal mol^{-1}, which indicates an additional 1.5 kcal mol^{-1} stabilization of the thiolate

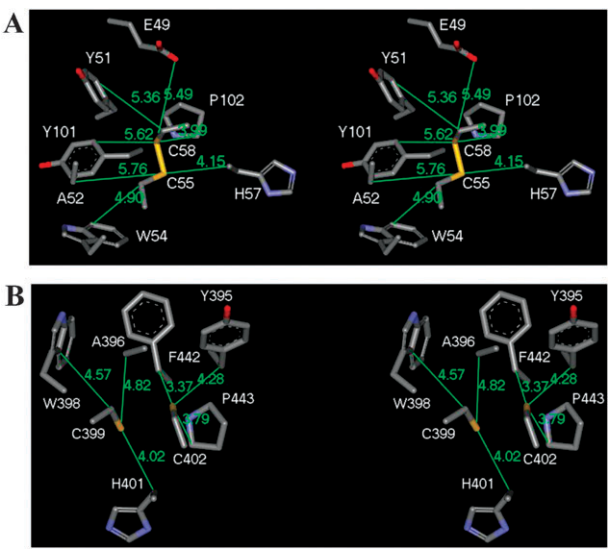

Fig. 9 Features of the surroundings of the reactive disulfide/thiols in PDI. Stereo view of the neighbours of the disulfide of bovine PDI *a*-domain (A) and *a*′-domain (B).

through electrostatic interaction. On the other hand, the negative charge on P34D manifests a small increase in pK_a compared to P34A, translating to a net repulsion of 0.1 kcal mol^{-1}.

Redox potential

All three mutations increase $E^{o\prime}$ compared to the wild-type, with the effect of the P34K mutation being the largest (28 mV), and P34D being the smallest (16 mV). $E^{o\prime}$ of P34A is 4 mV higher than that of P34D. The results are consistent with the relationship between pK_a and $E^{o\prime}$, a lower pK_a is correlated with a higher $E^{o\prime}$.[7] Therefore, Pro at the C-terminal X imparts a lowest $E^{o\prime}$ to Trx through avoidance of the amide–sulfur hydrogen bonding. Introducing this hydrogen bond increases $E^{o\prime}$ by 20 mV, as manifested in the P34A substitution. $E^{o\prime}$ values are also modulated by the electrostatic property of the C-terminal X. A negative charged residue at the C-terminal X gives a smaller increment, and a positively charged residue greatly increases $E^{o\prime}$. The results are in contrast to those of the N-terminal X, where the replacement of Gly by charged Lys or Asp has little effect on the $E^{o\prime}$ of Trx.[14,31]

Redox activities

Despite the importance of the nucleophilic pK_a and $E^{o\prime}$, the activities of Trx toward TrxR, insulin, and PDI did not follow pK_a and $E^{o\prime}$. In general, the redox activities of the P34K mutant are less affected than those of P34D, while the activity of P34A is closest to that of the wild-type. The rate of TrxR catalyzed reduction of Trx fell 96%, and that of insulin and PDI reduction decreased by 583-fold and 15-fold due to the P34D mutation. The results indicate that a negatively charged residue much more severely impedes the activity of Trx than a positively charged residue at the C-terminal X.

Kinetics and protein interaction

The major factor determining the redox reactivity can be observed from kinetic experiments. The change in rate of the Trx reduction catalyzed by TrxR is solely affected by the K_m, an indicator of protein interaction. The second order rate constants of the stoichiometric oxidoreductive reactions of Trx with insulin and with PDI are large for the wild-type Trx and significantly lower for the mutants. The multiple turnover experiments for the reduction of Trx and the reduction of insulin indicate that although k_{cat} affects the reactivity, a significant proportion of the high reactivity is attributed to K_m. Molecular modeling agrees with this conclusion (Fig. 4, 7 and 9). TrxR has a negatively charged interface, and the reaction rates were P34K > P34A > wild type > P34D. Both insulin and PDI carry a hydrophobic interface, and the reaction rates were wild-type > P34A > P34K > P34D. Because the ranks of pK_a and $E^{o\prime}$ were wild-type > P34D > P34A > P34K, the inconsistency between the ranks of reactivity and those of pK_a and $E^{o\prime}$ further demonstrates the importance of protein interaction in determining the reactivity. Substitutions of the N-terminal X with charged amino acids also manifested significant effects on K_m of redox reactions, supporting the importance of protein interaction.[14,31]

Implication to PDI-like proteins

The above observations can be used in analysis of other proteins with Trx-like domains. Yeast Eps1 interacts with a misfolded H^+-ATPase mutant, Pma1-D378N. The interaction requires the C_{60}PHC motif.[15] Another C_{200}DKC motif cooperates in recognition. The role of the charged residues in the CDKC motif has not been investigated. As the present study shows that the C-terminal X is important for protein interaction, the charged C-terminal X substitution of Eps1 may also assist in the interaction with Pma1-D378N or other target proteins. Interactions of TMX2 with other proteins have not been reported. The lack of nucleophilic Cys and the presence of charged C-terminal X suggest the involvement of the motif in the protein interaction. PDILT interacts with Ero1α, Δ-somatostatin, nonnative BPTI, and calmegin.[17,32] PDILT is redox inactive.[32] In view of the importance of the C-terminal X in affecting protein interaction, the charged substitutions in PDILT and TMX2 likely participate in interaction with specific proteins.

Conservation of pro at C-terminal X of Trx

Substitution of Lys and Ala for Pro34 in Trx increases the catalytic efficiency of TrxR 2.3-fold and 1.4-fold, respectively, mainly by lowering the K_m. It indicates that this position is important for protein–protein interaction, and amino acid replacement can facilitate the interaction with TrxR. Thus, the conservation of Pro in the wild-type Trx is not optimized for TrxR, but is favored for other purposes. The data on protein interaction, $E^{o\prime}$, and pK_a demonstrate that the C-terminal X crucially affects these properties. As Trx also serves as an electron donor for multiple proteins, a compromise in maintaining suitable $E^{o\prime}$ and pK_a, and the interaction with all client proteins including TrxR can exert a pressure for preserving Pro at C-terminal X during evolution.

Reaction mechanism

Oxidoreduction between thiol-disulfide oxidoreductases and substrate proteins has been generally described as a simple S_N2 reaction without the prior formation of a protein complex.[33,1,2] For a S_N2 redox reaction, the rate constant can be estimated from the equation of Szajewski and Whitesides.[34]

$$\log k' = (7.0 + 0.5pK_a^{nuc} - 0.27pK_a^{c} - 0.73pK_a^{lg}) - \log(1 + 10^{(pK_a^{nuc} - pH)}) \quad (1)$$

Where pK_a^{nuc}, pK_a^{c}, and pK_a^{lg} denote the pK_a of the nucleophilic, central, and leaving groups. Eqn (1) can not lead to rate constants as high as observed in the wild-type Trx of the present assays. Also, the changes in the rate constant k' between the wild-type and mutants would be at most 2.4-fold when Trx serves as a nucleophile in a S_N2 reaction. Both the observed high rate constants and the large variation of the measured rates between the wild-type and the mutants point to the large effect of protein–protein interaction.

The rate enhancement by protein interaction in the reduction of insulin is estimated as an example. The rate constant of reduction of insulin by DTT (pK_a = 9.2)[34] is 5 M^{-1} s^{-1}.[3] The estimated k_{app} for the wild-type Trx due to a pK_a^{nuc} = 7.6

would be only 25 M^{-1} s^{-1} at pH 7. The observed 1.4 × 10^5 M^{-1} s^{-1} suggests a prodigious rate enhancement due to the protein–protein interaction.

Although the S_N2 mechanism describes the chemistry, an additional step of noncovalent complex formation due to protein–protein interaction in the reaction mechanism better accounts for the observed reaction rates and mutational effects,

$$PA_{SH}^{SH} + PB_{S}^{S} \underset{k_{-1}}{\overset{k_1}{\longleftrightarrow}} PA_{SH}^{SH} \bullet {}_{S}^{S}PB \underset{k_{-2}}{\overset{k_2}{\longleftrightarrow}} PA_{SH}^{-S-S-}{}_{HS}PB \underset{k_{-3}}{\overset{k_3}{\longleftrightarrow}} PA_{S}^{S} + PB_{SH}^{SH} \quad (2)$$

where *PA* refers to the oxidoreductase, and *PB* is the substrate protein, or *vice versa* if the oxidoreductase is in the oxidized state. *SH* includes thiol and thiolate species. The reduced PA_{SH}^{SH} and the oxidized PB_{S}^{S} interact to form a noncovalent complex, $PA_{SH}^{SH}\cdot{}_{S}^{S}PB$. Subsequently, the attack by the thiolate of the nucleophilic Cys in *PA* on the disulfide of *PB* results in a covalent-mixed disulfide intermediate, $PA_{SH}^{-S-S-}{}_{HS}PB$. The other active site Cys of *PA* then reduces the disulfide bridge, thereby forming the product PB_{SH}^{SH}.

In the Trx redox system, the oxidized *PA* (Trx) produced in eqn (2) will be reduced again by another system component *C* (NADPH) under the catalysis of another enzyme (TrxR), eqn (3), yielding an overall reaction as shown by eqn (4).

$$PA_{S}^{S} + C_{\text{red}} \overset{k_4}{\longleftrightarrow} PA_{SH}^{SH} + C_{ox} \quad (3)$$

$$C_{\text{red}} + PB_{S}^{S} \leftrightarrow C_{ox} + PB_{SH}^{SH} \quad (4)$$

where C_{red} and C_{ox} refer to the reduced and oxidized component *C*.

Redox couples or redox enzymes

Whether redoxins should be described as redox couples or redox enzymes, which is essential knowledge for system biology study, has been questioned, and Michaelis–Menten parameters were considered as inappropriate descriptors of redoxin activity.[35] A Michaelis–Menten kinetic pattern as in Fig. 6 can arise from two possibilities, a redoxin serving as a redox couple or as an enzyme in a redox system, which complicates the distinction.[35] P34K, being 2.3-fold better for the TrxR catalyzed reaction while 40-fold worse for insulin reduction compared to the wild-type, provides a distinction of the reaction mechanism. For Trx working as a redox couple, the rate of insulin reduction in the Trx system is as follows,[35]

$$v = \frac{(k_4 ca)b}{(k_4 c/k_f) + b} \quad (5)$$

where k_4 is the rate constant of the TrxR catalyzed reaction (eqn (3)), and k_f is the forward rate constant for the reduction of insulin by Trx (Reduced Trx + insulin $\overset{k_f}{\longleftrightarrow}$oxidized Trx + reduced insulin). The concentrations of NADPH, the reduced Trx, and insulin are represented by *c*, *a*, and *b*, respectively. Hence, the ratio of the V_m between P34K and the wild-type is the ratio of k_4, and the ratio of K_m between P34K and the wild-type is the ratio of k_4/k_f for these two Trx. Accordingly, V_m for the reduction of insulin by P34K should be 2.3-fold larger than that by the wild-type if Trx is a redox couple. The current experimental data does not show this large increment of V_m. On the contrary, the V_m for P34K is 3.8-fold lower compared to the wild-type value. Similarly, K_m will be 92-fold larger for P34K relative to the K_m for the wild-type if Trx is a redox couple. The experimental K_m for P34K is only 5.6-fold larger than the wild-type value. These large discrepancies reveal that Trx is not a redox couple (Fig. 10). Furthermore, when reduction of insulin by the wild-type Trx was performed at one half of the NADPH concentration, the K_m was 12.8 μM and V_m was 4.9 μM min^{-1} (Fig. 6). K_m and V_m did not reduce to one half, as would have been expected if Trx acts as a redox couple. Therefore, in a complete redox system, Trx works as an enzyme. It is therefore inferred that oxidoreduction of proteins by Trx can be described by the current proposed mechanism shown in eqn (2).

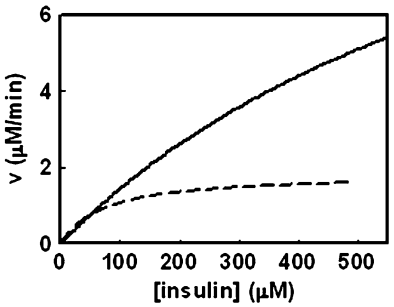

Fig. 10 Insulin reduction by P34K Trx in the Trx system. Solid line, modeled based on P34K being a redox couple, V_m = 13.11 μM min^{-1}, K_m = 948 μM; dashed line, regression curve for P34K experimental data in Fig. 6.

Redox reactions against $E^{o\prime}$

The key role of protein–protein interaction in powering the redox reactivity may provide an explanation for why redox proteins can effectively carry out oxidoreduction of thiol/disulfide in a direction opposite to that prescribed by pK_a or $E^{o\prime}$ in certain puzzling observations. For instance, the most reductive Trx, exported to the periplasm, can oxidize thiols of periplasmic proteins,[36] and the most oxidative DsbA is oxidized rapidly (k = 2.7 × 10^6 M^{-1} s^{-1}) by the more reducing DsbB.[37] The interaction between proteins facilitates a faster reaction, and thermodynamically the reaction can be further driven favorably by coupling to the upstream and/or downstream electron flow in the complete redox cascade. Therefore, the present proposed mechanism can rationalize the inexplicable behaviors of redox proteins by a consistent framework.

Experimental

Preparation of mutant Trx

The P34D and P34K mutants were obtained by sequential PCR using a plasmid carrying wild-type Trx, pET/WT, as a template.[31] In the first PCR, the plasmid was amplified with the primer 5′-TGATGGTGCATAAGGCCTGAACCAGATCAG-3′ and one of the following: 5′-TGCGGT*GAC*TGCAAAATGATCGC-3′ (P34D), or 5′-TGCGGT*AA*GTGCAAAATGATC-3′ (P34K). The mismatched bases are listed in

italics. The PCR product and 5′-TAATACGACTCACTA-TAGGG-3′ (T7) were then used as primers for the second PCR. The amplification product was digested with *Xba*I and *Stu*I, and ligated back to the vector to obtain pET/P34K and pET/P34D. P34A was amplified from a Trx bearing plasmid pKS/WT with primers 5′-TGCGGT*G*CGTGCAAAATGATC-3′ (P34A) and T7. The product and a primer of 5′-ATTAAC-CCTCACTAAAGGGA-3′ (T3) were used for the second PCR. The amplified fragment was ligated to pGEM-T easy vector, digested by *Nde*I and *Bam*H1, and then ligated to pET vector to generate pET/P34A. The mutant genes were confirmed by dideoxy sequencing. Proteins were expressed and purified following the published procedures.[31]

Fluorescence spectra of the wild-type and mutant Trx

Fluorescence spectra of 7 μM Trx in 0.05 M sodium phosphate, pH 7.5, were recorded at 25 °C using a Hitachi F-4500 spectrofluorimeter with an excitation wavelength of 295 nm. Solvent control was subtracted. The reduced proteins were measured in the presence of 0.13 mM DTT. Trx concentrations were determined with ε_{280} of 13700 M^{-1} cm^{-1}.

pK_a determination

The pK_a of thiols in Trx was determined from the variation of ε_{240} with pH at 25 °C.[29] Reduced Trx was prepared before use by incubating 0.1–0.2 mM of the purified protein with 40 mM DTT in 0.1 M Tris-HCl, pH 7.5, and purified by a Sephadex G25 column. The UV absorbance of 6–11 μM of reduced Trx was measured in a buffer containing 1 mM of phosphate, borate, and citrate, 0.2 M KCl, and 0.1 mM EDTA, adjusted to various pH. For P34D, P34A and P34K, the pH dependent change of ε_{240} was fitted to the Henderson–Hasselbalch equation. The pK_a of the wild-type Trx was determined following the theory of the microscopic deprotonation constants K_1 and K_2 of two interacting monoprotic species,[38] assuming the equivalence of ε_{HB} and ε_{HH},

$$\varepsilon = \frac{\varepsilon_{HH}[H^+]^2 + \varepsilon_{HB}K_1[H^+] + \varepsilon_{BH}K_2[H^+] + c\varepsilon_{BB}K_1K_2}{[H^+]^2 + K_1[H^+] + K_2[H^+] + cK_1K_2}$$

where ε_{HH}, ε_{HB}, ε_{BH}, ε_{BB} are the extinction coefficients of the doubly protonated, two singly protonated, and the double deprotonated species, respectively, and c is a coefficient.

Redox equilibrium constant and redox potential

Thiol to disulfide redox equilibrium constant (K) of Trx was measured with reference to glutathione as described earlier,[9,31] and $E^{o\prime}$ was then obtained from the Nernst equation, using a $E^{o\prime}$ of −0.240 V for glutathione. Data shown are the mean ± SD of three experiments.

Reduction of Trx catalyzed by TrxR

Initial rates of NADPH-dependent reduction of Trx were measured in a buffer comprising 0.08 mg ml^{-1} bovine serum albumin, 0.5 mM 5,5′-dithiobis(2-nitrobenzoic acid) (DTNB), 0.1 M sodium phosphate, 2 mM EDTA, pH 7.0. Each assay contained 0.24 mM NADPH, 5.4 nM TrxR, and oxidized Trx in amounts of 0.09–5.01 μM for the wild-type, 0.14–8.72 μM for P34K, 0.6–220 μM for P34D, and 0.09–7.05 μM for P34A. The change in absorbance at 412 nm with respect to a reference cuvette under otherwise identical conditions except for the absence of Trx was recorded at 25 °C. The production of thionitrobenzoate was calculated with ε_{412} of 13 600 M^{-1} cm^{-1}. The mean ± SD of three experiments was reported.

Reduction of insulin by Trx

Assays of insulin reduction using Trx as a stoichiometric reductant followed the procedure of Krause *et al.* with some modification.[8] Reduced Trx at a concentration of 0.5–1 μM was supplied to a nitrogen purged solution of 0.1 M sodium phosphate, 2 mM EDTA, pH 7, and then bovine insulin (Sigma-Aldrich Co., St. Louis, MO) was added to the same concentration as Trx. Insulin concentration was determined from the absorbance with an absorption coefficient at 278 nm of 1.03 Lg^{-1} cm^{-1}.[39] The reaction mix was thermostated at 15 °C, and the fluorescence change was followed at 350 nm using excitation wavelength of 300 nm. To show that Trx retained the redox activity, DTT was added to the mixture to 1 mM final concentration. The initial rate of oxidation of Trx was used to obtain the apparent second order rate constant (k_{app}) by taking the concentrations of the Trx and insulin to be the same. Reduction of insulin by the Trx system was measured as described by Holmgren.[3] The reaction mixture consisted of 0.4 mM NADPH, 0.1 μM Trx, and insulin in 0.1 M sodium phosphate, 2 mM EDTA, pH 7. The reaction was started by adding 110 nM of TrxR, and the absorbance was monitored at 340 nm at 25 °C. A reaction mixture that contained the same components except insulin was used as a reference. Experiments were performed with different concentrations of insulin each time. Data shown are the mean ± SD.

Oxidation of Trx by PDI

Oxidation of Trx was performed by adding reduced Trx to a nitrogen purged solution composed of bovine PDI (Sigma-Aldrich Co., St. Louis, MO) in 0.1 M sodium phosphate, 2 mM EDTA, pH 7, as described by Lundstrom and Holmgren.[26] The final concentrations of PDI and Trx were 0.5 μM, and the reaction was monitored by fluorescence at 350 nm at 25 °C, using excitation of 300 nm. Concentration of PDI was determined with an ε_{280} of 47 300 M^{-1} cm^{-1}. The fluorescence intensity of a solution containing PDI alone was investigated, and it did not change after reduction by DTT. For checking of the redox activity of Trx in the solution, insulin was added to 0.33 μM, and finally 2 mM DTT was delivered. The apparent rate constant, k_{app}, was evaluated from the initial rate of Trx oxidation using equal concentrations of the reactants. The mean ± SD of three experiments was reported.

Modeling of proteins

Alignment of bovine and human PDI *a*-domain and *a*′-domain sequences was based on ClustalW.[40] These two species share 96% and 99% sequence identity for the *a*-domain and *a*′-domain, respectively (Fig. S2†). Human PDI *a*-domain (PDB entry 1MEK) and *a*′-domain (PDB entry 1X5C) were adopted as templates for homology modeling of the bovine domain structures, and the structures were refined by energy minimization and molecular dynamics with GROMOS96.[41] The RMS for the optimized bovine *a* and *a*′-domain structures

are 0.11 Å and 0.07 Å, respectively, in the backbone atoms. The protein structures, solvent accessibilities, surface properties, and contact distances were prepared with MOLMOL[42] and WebLab Viewer Lite (Accelrys). The structural change of Trx in complex with TrxR due to mutation of Trx was confined to the position of mutation and refined by GROMOS96.

Electrophoresis

Sodium dodecyl sulfate polyacrylamide gel electrophoresis (SDS-PAGE) was performed to analyze the reduced and denatured proteins in 15% SDS-PAGE gel. Native gel electrophoresis for Trx was performed on 15% polyacrylamide gel under a nondenaturing condition. Protein bands were visualized by Coomassie Blue staining.

Acknowledgements

This work was partially supported by NSC (95-2311-B-009-003). The author thanks Dr C. W. Lin for suggestions on the manuscript.

References

1 C. Berndt, C. H. Lillig and A. Holmgren, *Am. J. Physiol.: Heart Circ. Physiol.*, 2007, **292**, H1227–1236.
2 C. Appenzeller-Herzog and L. Ellgaard, *Biochim. Biophys. Acta, Mol. Cell Res.*, 2008, **1783**, 535–548.
3 A. Holmgren, *J. Biol. Chem.*, 1979, **254**, 9113–9119.
4 K. W. Walker and H. F. Gilbert, *Biochemistry*, 1995, **34**, 13642–13650.
5 S. K. Katti, D. M. LeMaster and H. Eklund, *J. Mol. Biol.*, 1990, **212**, 167–184.
6 M. Huber-Wunderlich and R. Glockshuber, *Folding Des.*, 1998, **3**, 161–171.
7 P. T. Chivers, K. E. Prehoda and R. T. Raines, *Biochemistry*, 1997, **36**, 4061–4066.
8 G. Krause, J. Lundstrom, J. L. Barea, C. Pueyo de la Cuesta and A. Holmgren, *J. Biol. Chem.*, 1991, **266**, 9494–9500.
9 T. Y. Lin and P. S. Kim, *Biochemistry*, 1989, **28**, 5282–5287.
10 J. Lundstrom and A. Holmgren, *Biochemistry*, 1993, **32**, 6649–6655.
11 A. Zapun, J. C. Bardwell and T. E. Creighton, *Biochemistry*, 1993, **32**, 5083–5092.
12 S. Quan, I. Schneider, J. Pan, A. Von Hacht and J. C. Bardwell, *J. Biol. Chem.*, 2007, **282**, 28823–28833.
13 U. Grauschopf, J. R. Winther, P. Korber, T. Zander, P. Dallinger and J. C. Bardwell, *Cell*, 1995, **83**, 947–955.
14 T. Y. Lin and T. S. Chen, *Biochemistry*, 2004, **43**, 945–952.
15 Q. Wang and A. Chang, *EMBO J.*, 2003, **22**, 3792–3802.
16 X. Meng, C. Zhang, J. Chen, S. Peng, Y. Cao, K. Ying, Y. Xie and Y. Mao, *Biochem. Genet.*, 2003, **41**, 99–106.
17 M. van Lith, N. Hartigan, J. Hatch and A. M. Benham, *J. Biol. Chem.*, 2005, **280**, 1376–1383.
18 B. W. Lennon, C. H. Williams, Jr. and M. L. Ludwig, *Science*, 2000, **289**, 1190–1194.
19 D. Y. Lee, B. Y. Ahn and K. S. Kim, *Biochemistry*, 2000, **39**, 6652–6659.
20 S. J. Jeon and K. Ishikawa, *Eur. J. Biochem.*, 2002, **269**, 5423–5430.
21 M. Akif, G. Khare, A. K. Tyagi, S. C. Mande and A. A. Sardesai, *J. Bacteriol.*, 2008, **190**, 7087–7095.
22 A. Lewin, A. Crow, C. T. Hodson, L. Hederstedt and N. E. Le Brun, *Biochem. J.*, 2008, **414**, 81–91.
23 J. Kemmink, N. J. Darby, K. Dijkstra, M. Nilges and T. E. Creighton, *Curr. Biol.*, 1997, **7**, 239–245.
24 J. S. Weissman and P. S. Kim, *Nature*, 1993, **365**, 185–188.
25 G. D. Smith, W. A. Pangborn and R. H. Blessing, *Acta Crystallogr., Sect. D: Biol. Crystallogr.*, 2005, **61**, 1476–1482.
26 J. Lundstrom and A. Holmgren, *J. Biol. Chem.*, 1990, **265**, 9114–9120.
27 N. A. Morjana and H. F. Gilbert, *Biochemistry*, 1991, **30**, 4985–4990.
28 V. Westphal, J. C. Spetzler, M. Meldal, U. Christensen and J. R. Winther, *J. Biol. Chem.*, 1998, **273**, 24992–24999.
29 T. Kortemme and T. E. Creighton, *J. Mol. Biol.*, 1995, **253**, 799–812.
30 N. Foloppe, J. Sagemark, K. Nordstrand, K. D. Berndt and L. Nilsson, *J. Mol. Biol.*, 2001, **310**, 449–470.
31 T. Y. Lin, *Biochemistry*, 1999, **38**, 15508–15513.
32 M. van Lith, A. R. Karala, D. Bown, J. A. Gatehouse, L. W. Ruddock, P. T. Saunders and A. M. Benham, *Mol. Biol. Cell*, 2007, **18**, 2795–2804.
33 A. T. Carvalho, P. A. Fernandes, M. Swart, J. N. Van Stralen, F. M. Bickelhaupt and M. J. Ramos, *J. Comput. Chem.*, 2009, **30**, 710–724.
34 R. P. Szajewski and G. M. Whitesides, *J. Am. Chem. Soc.*, 1980, **102**, 2011–2026.
35 C. S. Pillay, J. H. Hofmeyr, B. G. Olivier, J. L. Snoep and J. M. Rohwer, *Biochem. J.*, 2009, **417**, 269–275.
36 L. Debarbieux and J. Beckwith, *Proc. Natl. Acad. Sci. U. S. A.*, 1998, **95**, 10751–10756.
37 U. Grauschopf, A. Fritz and R. Glockshuber, *EMBO J.*, 2003, **22**, 3503–3513.
38 P. T. Chivers, K. E. Prehoda, B. F. Volkman, B. M. Kim, J. L. Markley and R. T. Raines, *Biochemistry*, 1997, **36**, 14985–14991.
39 G. Vecchio, A. Bossi, P. Pasta and G. Carrea, *Int. J. Pept. Protein Res.*, 1996, **48**, 113–117.
40 W. R. Pearson and D. J. Lipman, *Proc. Natl. Acad. Sci. U. S. A.*, 1988, **85**, 2444–2448.
41 S. R. Billeter, W. F. van Günsteren, A. A. Eising, P. H. Hünenberger, P. Krüger, A. E. Mark, W. R. P. Scott and I. G. Tironi, *Biomolecular simulation: The GROMOS96 manual and user guide*, Vdf Hochschulverlag AG an der ETH Zürich, Zürich, Switzerland, 1996.
42 R. Koradi, M. Billeter and K. Wuthrich, *J. Mol. Graph*, 1996, **14**, 51–55.

